RESEARCH PAPER

Mexiletine as a treatment for primary erythromelalgia: normalization of biophysical properties of mutant L858F Na$_V$1.7 sodium channels

R Cregg[1,2], J J Cox[1], D L H Bennett[3], J N Wood[1] and R Werdehausen[1,4]

[1]*Molecular Nociception Group, Wolfson Institute for Biomedical Research, UCL, London, UK,*
[2]*UCL Centre for Anaesthesia, Critical Care and Pain Medicine, London, UK,* [3]*The Nuffield Department of Clinical Neuroscience, University of Oxford, UK, and* [4]*Department of Anesthesiology, Medical faculty, Heinrich-Heine-University, Düsseldorf, Germany*

BACKGROUND AND PURPOSE

The non-selective sodium channel inhibitor mexiletine has been found to be effective in several animal models of chronic pain and has become popular in the clinical setting as an orally available alternative to lidocaine. It remains unclear why patients with monogenic pain disorders secondary to gain-of-function SCN9a mutations benefit from a low systemic concentration of mexiletine, which does not usually induce adverse neurological side effects. The aim of this study was, therefore, to investigate the biophysical effects of mexiletine on the L858F primary erythromelalgia Na$_V$1.7 mutation *in vitro*.

EXPERIMENTAL APPROACH

Human wild-type and L858F-mutated Na$_V$1.7 channels were expressed in HEK293A cells. Whole-cell currents were recorded by voltage-clamp techniques to characterize the effect of mexiletine on channel gating properties.

KEY RESULTS

While the concentration-dependent tonic block of peak currents by mexiletine was similar in wild-type and L858F channels, phasic block was more pronounced in cells transfected with the L858F mutation. Moreover, mexiletine substantially shifted the pathologically-hyperpolarized voltage-dependence of steady-state activation in L858F-mutated channels towards wild-type values and the voltage-dependence of steady-state fast inactivation was shifted to more hyperpolarized potentials, leading to an overall reduction in window currents.

CONCLUSION AND IMPLICATIONS

Mexiletine has a normalizing effect on the pathological gating properties of the L858F gain-of-function mutation in Na$_V$1.7, which, in part, might explain the beneficial effects of systemic treatment with mexiletine in patients with gain-of-function sodium channel disorders.

Abbreviations

A/D, analogue to digital; E_{rev}, reversal potential; I, current; Na$_V$, voltage-gated sodium channel; PEM, primary erythromelalgia; WT, wild type

Table of Links

TARGETS	LIGANDS
Na_V	Mexiletine
$Na_V1.7$	Lidocaine

This Table lists key protein targets and ligands in this document, which are hyperlinked to corresponding entries in http://www.guidetopharmacology.org, the common portal for data from the IUPHAR/BPS Guide to PHARMACOLOGY (Pawson et al., 2014) and are permanently archived in the Concise Guide to PHARMACOLOGY 2013/14 (Alexander et al., 2013).

Introduction

The non-selective sodium channel inhibitor mexiletine hydrochloride [1-methyl-2-(2,6-xylyloxy)ethylamine hydrochloride] has been extensively studied and used clinically for decades because of its antiarrhythmic effects (Chew et al., 1979; Woosley et al., 1984; Fenster and Comess, 1986; Monk and Brogden, 1990). More recently, it has also been found to be effective in several animal models of chronic pain and it has been suggested as a third-line treatment instead of systemic lidocaine for neuropathic pain syndromes (Jarvis and Coukell, 1998; Kuhnert et al., 1999; Mao and Chen, 2000; Challapalli et al., 2005; Tremont-Lukats et al., 2005; Ebell, 2006; Marmura, 2010). Based on its almost complete absorption after oral administration, its low first-pass effect and a plasma elimination half-life of approximately 10–14 h, it is also an orally available alternative to lidocaine for systemic treatment (Middleton, 1980).

Recently, it has been noted that systemic treatment with mexiletine alleviates the symptoms and signs of myotonia in non-dystrophic myotonia (Statland et al., 2012). Non-dystrophic myotonia results from mutations in the voltage-gated sodium channel encoded by the gene SCN4A (Matthews et al., 2010). In comparison, gain-of-function mutations in the related SCN9A gene, which encodes $Na_V1.7$, can result in primary erythromelalgia (PEM), either a familial or a sporadic chronic neuropathic pain syndrome (Dib-Hajj et al., 2005). Several publications have reported an analgesic effect of mexiletine in patients suffering from this monogenic pain disorder (Kuhnert et al., 1999; Legroux-Crespel et al., 2003; Dib-Hajj et al., 2005; Nathan et al., 2005; Choi et al., 2009). The apparent absence of pro-arrhythmic and other major adverse effects at analgesic doses of mexiletine points to a mode of action that preferentially affects pathological channels. While a pronounced use-dependent sodium channel block in an erythromelalgia-causing $Na_V1.7$ mutation has been demonstrated before (Choi et al., 2009), the mechanisms that lead to the observed analgesic effect are not fully understood. The L858F mutation in $Na_V1.7$ is one of the best characterized and most common gain-of-function mutations that leads to PEM and is associated with a severe phenotype (Han et al., 2007; Samuels et al., 2008; Cheng et al., 2011; Segerdahl et al., 2012). The 858 residue is located near the pore region within the second domain of $Na_V1.7$ (Figure 1A). Sequence alignment of voltage-gated sodium
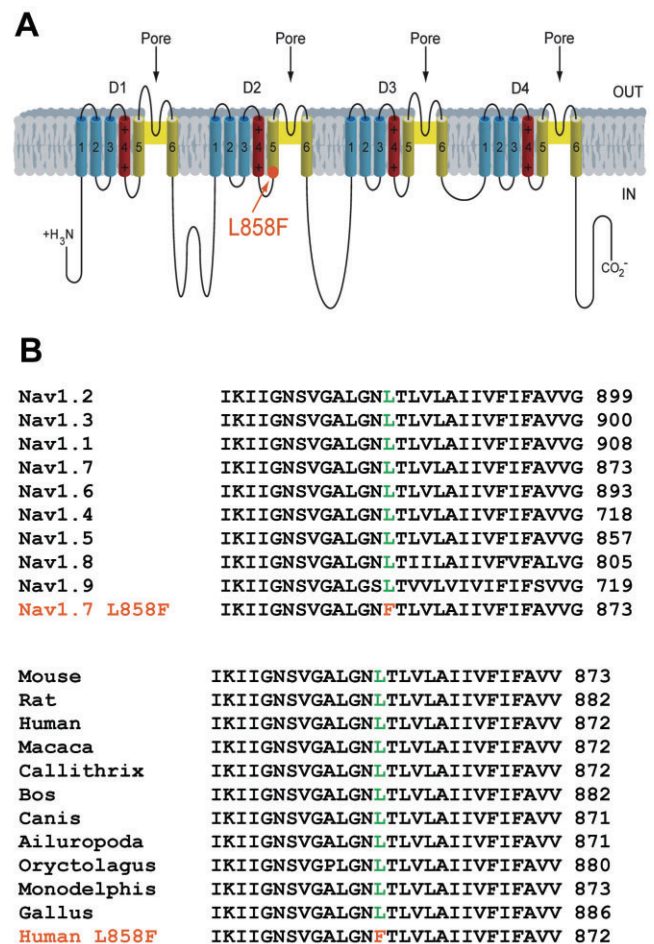

Figure 1

(A) Diagram of $Na_V1.7$ showing the location of the p.L858F amino acid substitution. p.L858F maps to the S4–S5 intracellular linker of domain 2 and is identified by the orange solid circle and the arrow. (B) Amino acid residue alignment around p.L858F. Amino acid residue alignment demonstrating the magnitude of inter-isoform and inter-species conservation of the affected regions. Orange residues identify the mutant p.L858F mapping to the S4–S5 linker of DII of the human $Na_V1.7\alpha$ subunit. Green colour indicates the corresponding non-mutated variant.

channels (Na$_V$s) shows that the leucine at position 858 is individually conserved in every member of the Na$_V$ family in humans and highly evolutionarily conserved in all Na$_V$1.7 homologues (Figure 1B). It has previously been shown that the L858F mutation causes a hyperpolarizing shift in the voltage- dependence of steady-state fast activation and an enhanced response to slow depolarizations (Han *et al.*, 2006).

Therefore, the aim of this study was to investigate the biophysical effects of mexiletine on the PEM-causing L858F Na$_V$1.7 mutation *in vitro*, with particular focus on channel gating properties. A better understanding of how mexiletine affects the gating properties of a pathologically dysfunctional channel may enable research to focus on specific gating properties of this channel for future drug development. Thus, we expressed human Na$_V$1.7 channels with or without the L858F mutation in HEK293A cells and analysed the effect of mexiletine on their whole-cell voltage-clamp properties.

Methods

Plasmid and site-directed mutagenesis

A previously described full-length human SCN9A cDNA sequence cloned into a modified pcDNA3 expression vector containing downstream polio IRES and DsRED2 sequences (FLRED) was used (Cox *et al.*, 2006). The L858F mutation was introduced into FLRED using the QuikChange II XL Site-Directed Mutagenesis Kit (Stratagene, La Jolla, CA, USA) according to the manufacturer's instructions. The coding sequence of both constructs was fully sequenced to verify the desired mutation and to ensure that no other variations had been introduced.

Cell culture and transfection

HEK293A cells were cultured in a humidified atmosphere containing 5% carbon dioxide at 37°C and were grown in DMEM (Gibco, Life Technologies, Carlsbad, CA, USA) supplemented with 10% heat-inactivated FBS. Unless stated otherwise, reagents were purchased from Sigma Aldrich (St. Louis, MO, USA).

Cells were transiently transfected with plasmid DNA for expression of Na$_V$1.7 human wild-type (WT) α subunits (Ref Seq NM_002977) or L858F-mutated α subunits (SCN9A-IRES-DsRed2 in pcDNA3 vector) combined with human WT β1 (Ref Seq NM_001037) and β2 (Ref Seq NM_001037) subunits (SCN1B-IRES-SCN2B-IRES-eGFP in a pIRES2-AcGFP1 backbone vector) as previously described (Cox *et al.*, 2006). In brief, transient transfection was performed with cells seeded at 80–90% confluency in 35 mm cell culture dishes using Lipofectamine 2000 (Invitrogen, Life Technologies) according to the manufacturer's recommendations. After 6 h, the transfection medium was replaced with fresh culture medium and the cells re-seeded for electrophysiological recordings at 20–30% confluency.

Electrophysiological recordings

Whole-cell membrane current recordings were performed 46–78 h after transfection. All recordings were made at room temperature. Micropipettes were pulled from borosilicate glass capillaries (GC150F-10; Harvard Apparatus, Kent, UK) using a Brown-Flaming P-97 horizontal micropipette puller

(Sutter Instruments, Novato, CA, USA, USA) and then fire polished on a microforge (MF-830 Narishige Group, Tokyo, Japan). Voltage errors were minimized with correction and prediction mode of series resistance compensation, both set to 50%. Extracellular (bath) solution contained (in mmol·L^{-1}): 140 NaCl, 4 KCl, 2 CaCl$_2$, 1 MgCl$_2$, 10 HEPES, adjusted to pH 7.4 with NaOH, osmolarity 320–325 mOsm·L^{-1} with glucose. Pipettes were filled with an intracellular solution containing (in mmol·L^{-1}): 140 CsCl, 5 NaCl, 5 EGTA, 2 MgCl$_2$, 10 HEPES adjusted to pH 7.3 with CsOH, osmolarity 305–310 mOsm·L^{-1} with glucose. Once filled with the appropriate intracellular solution, recording electrodes had a resistance between 2.0 and 3.2 MΩ. A silver chloride-coated silver wire served as a reference electrode with one end connected to the ground input of the amplifier and the tip placed directly into the bath solution. Cells having a leak current, after establishment of a whole-cell configuration, of more than 10% of the peak sodium current were discarded and those which had developed a leak current of this magnitude during the experiment were not used in the final analysis. The liquid junction potentials between the bath and the pipette solutions were not corrected. Whole-cell membrane currents were filtered at 5 kHz and sampled at 20 kHz using an Axopatch 200B patch clamp amplifier (Molecular Devices, Foster City, CA, USA) and Digidata 1200B A/D (analogue to digital) converter (Molecular Devices). Data were acquired on a Windows-based PC using Clampex (Molecular Devices) software and analysed by pCLAMP (Clampfit) 9.2 software (Molecular Devices).

Mexiletine treatment

Mexiletine hydrochloride salt was dissolved in extracellular (bath) solution to give a stock solution of 100 mM and pH was adjusted to 7.4. Subsequent dilutions were performed in a standard external solution to reach the desired concentrations. Addition of mexiletine did not change the osmolarity of the extracellular solution used in these experiments. For microperfusion with laminar flow at 1 mL·min^{-1}, a gravity-driven perfusion system (MEV-9, BioLogic Science Instruments, Claix, France) equipped with polyethylene tubing was used. The solution was removed using a Dymax 5 suctioning apparatus (Charles Austen Pumps Ltd., Byfleet, Surrey, UK). For concentration–response experiments, mexiletine was applied in a stepwise approach from the lowest to highest concentration, and 30 s was allowed after each concentration change for the response to reach a plateau before the effect induced was recorded.

Voltage-clamp protocols

To characterize the voltage-dependence of the steady-state channel activation, currents were evoked by voltage increments of 10 mV from –80 to +40 mV for 10 ms from a holding potential of –120 mV with 5 s between pulses. Conductance (*G*) values were calculated from the peak inward currents (*I*) measured and the reversal potential for sodium ions (*E*$_{rev}$ Na) observed using the equation $G = I/(V_m - E_{rev} Na)$.

Reversal potential was measured by extrapolating the linear portion of the *I/V* relationship between +10 and +40 mV. The resulting values for conductance were normalized to the peak conductance and fitted using the Boltzmann equation. Steady-state inactivation of WT Na$_V$1.7 channels or

L858F mutant channels was assessed by holding cells at increasing potentials from –110 to 0 mV for 500 ms, followed by a step to –10 mV for 50 ms.

For characterization of the use-dependence of mexiletine-induced block in $Na_V1.7$ WT and L858F variant channels, currents were elicited in whole-cell configuration by initially holding the cell at –120 mV and stepping up to 0 mV for 5 ms every 200 ms, generating pulses at a frequency of 5 Hz.

Statistical analysis

All data are expressed as means ± SEM. Differences in means between WT channels and mutations were tested by Student's two-tailed t-test or one-way ANOVA with the Bonferroni post test where appropriate. $P < 0.05$ was considered significant. Calculations were made using the GraphPad Prism software version 5.0 (GraphPad Software Inc., La Jolla, CA, USA).

Results

HEK293A cells transfected with the $Na_V1.7$ α subunit containing the L858F mutation ($n = 35$) in combination with the $Na_V\beta1$ and $Na_V\beta2$ subunits did not differ significantly from cells with WT Na_V 1.7 ($n = 29$) in terms of peak current densities and whole-cell capacity and series resistance (Table 1). The inhibition of WT and L858F channels by mexiletine was assessed by measuring the magnitude of the reduction in peak current achieved by depolarizing cells to 0 mV from a resting potential of –120 mV. Both peak currents (WT and L858F) were reduced in the presence of mexiletine in a concentration-dependent manner (Figure 2A). The fit of concentration–response curves with a first-order binding function revealed that the half-maximal blocking concentration (IC_{50}) was 1.1 ± 0.05 mM for the WT and 0.87 ± 0.06 mM for the L858F mutant channels.

Channels with the L858F mutations demonstrated a greater amount of use-dependent normalized peak current fall-off when compared with the WT in the presence of mexiletine (500 μM) when depolarized at a frequency of 5 Hz (Figure 2B and C). Comparing averaged currents recorded between pulse 10 and 20 with currents recorded between pulse 140 and 150, normalized peak current for cells expressing channels with the L858F mutation were reduced by 26%

($n = 8$; $P < 0.05$), while the effect of mexiletine on currents recorded from WT controls remained unchanged (Figure 2D).

In $Na_V1.7$ channels with the L858F mutation, the voltage-dependence of channel activation was found to be changed to more hyperpolarizing potentials compared with WT channels when normalized peak inward currents were plotted as a function of depolarization potential to demonstrate the current–voltage relationship (Figure 3A and B). When the resulting conductance values were fitted to a Boltzmann equation (Figure 3C), the L858F mutation caused a hyperpolarizing shift in the voltage-dependence of steady-state activation (Figure 3D; $P < 0.01$), with a voltage step leading to half-maximal activation ($V_{1/2act}$) of -19.7 ± 1.3 mV ($n = 20$) compared with -2.6 ± 1.3 mV ($n = 15$) in WT controls ($P < 0.01$). While mexiletine (500 μM) did not have an effect on the voltage-dependence of steady-state activation in WT $Na_V1.7$ channels (-5.0 ± 2.7 mV; $n = 9$), it shifted those of channels with the L858F mutation towards physiological values (-4.5 ± 3.3 mV) (Figure 3D; $n = 20$; $P < 0.01$). Furthermore, in L858F mutant channels, the slope of the function describing the voltage–conductance relationship was significantly changed by mexiletine (4.6 ± 0.7 vs. 8.5 ± 1.2; $P < 0.001$; Figure 3C), whereas it remained unchanged in $Na_V1.7$ WT channels (5.1 ± 0.2 vs. 5.4 ± 0.4).

When analysing the voltage-dependence of the steady-state fast inactivation (Figure 4), we found no difference in the voltages with half-maximal inactivation ($V_{1/2inact}$) between WT channels and those with the L858F mutation (-59.3 ± 3.1 and -56.5 ± 2.5 mV respectively). Mexiletine (500 μM) shifted the $V_{1/2inact}$ towards more hyperpolarized potentials for $Na_V1.7$ WT and L858F mutant channels (-77.3 ± 4.7 mV; $n = 14$; $P < 0.01$ and -73.0 ± 2.2 mV; $n = 15$; $P < 0.01$ respectively). The slope factors of fitted curves did not differ between L858F mutants and WT $Na_V1.7$.

A composite graph showing Boltzmann fits of mean activation and steady-state inactivation curves of L858F mutant versus WT channels showed an increase in the window current (Figure 5). Maximum window currents for WT $Na_V1.7$ channels were 4.5% of the peak currents (AUC = 0.82) as opposed to 11.5% seen in the mutant channel population of cells (AUC = 2.49). Following the application of mexiletine (500 μM) and after a steady state had been reached, there was a reduction in the maximum window current to 5.5% of peak currents in L858F channels and a reduction in the window current AUC by 48% (AUC = 1.29).

Table 1

Cell and recording properties

	Peak current (nA)	Whole-cell capacity (pF)	Series resistance (MΩ)
Controls ($n = 29$)	–0.68 (0.09)	16.8 (1.88)	12.7 (1.22)
L858F ($n = 35$)	–0.53 (0.08)	22.7 (1.90)	16.4 (1.99)
P value	0.08 (ns)	0.12 (ns)	0.11 (ns)

Data presented as mean values and SEM. Differences in means of cells with $Na_V1.7$ L858F mutant channels compared with $Na_V1.7$ wild-type controls were tested by Student's two-tailed t-test. $P < 0.05$ was considered significant.

Discussion

PEM is a devastating human disorder in which patients suffer from excruciating episodic pain, mainly in the hands and feet. A frequently used treatment for this disorder is the sodium channel blocker mexiletine. Here, we have studied the concentration- and frequency-dependent effects of mexiletine on $Na_V1.7$ channels with the erythromelalgia-associated mutation L858F, whose effect on channel properties as has been described previously (Han et al., 2007; Cheng et al., 2011). Intriguingly, mexiletine caused a change in the gating properties of this mutated channel, leading to an almost completely normalized voltage-dependence of activation and window currents, whereas the voltage-dependence
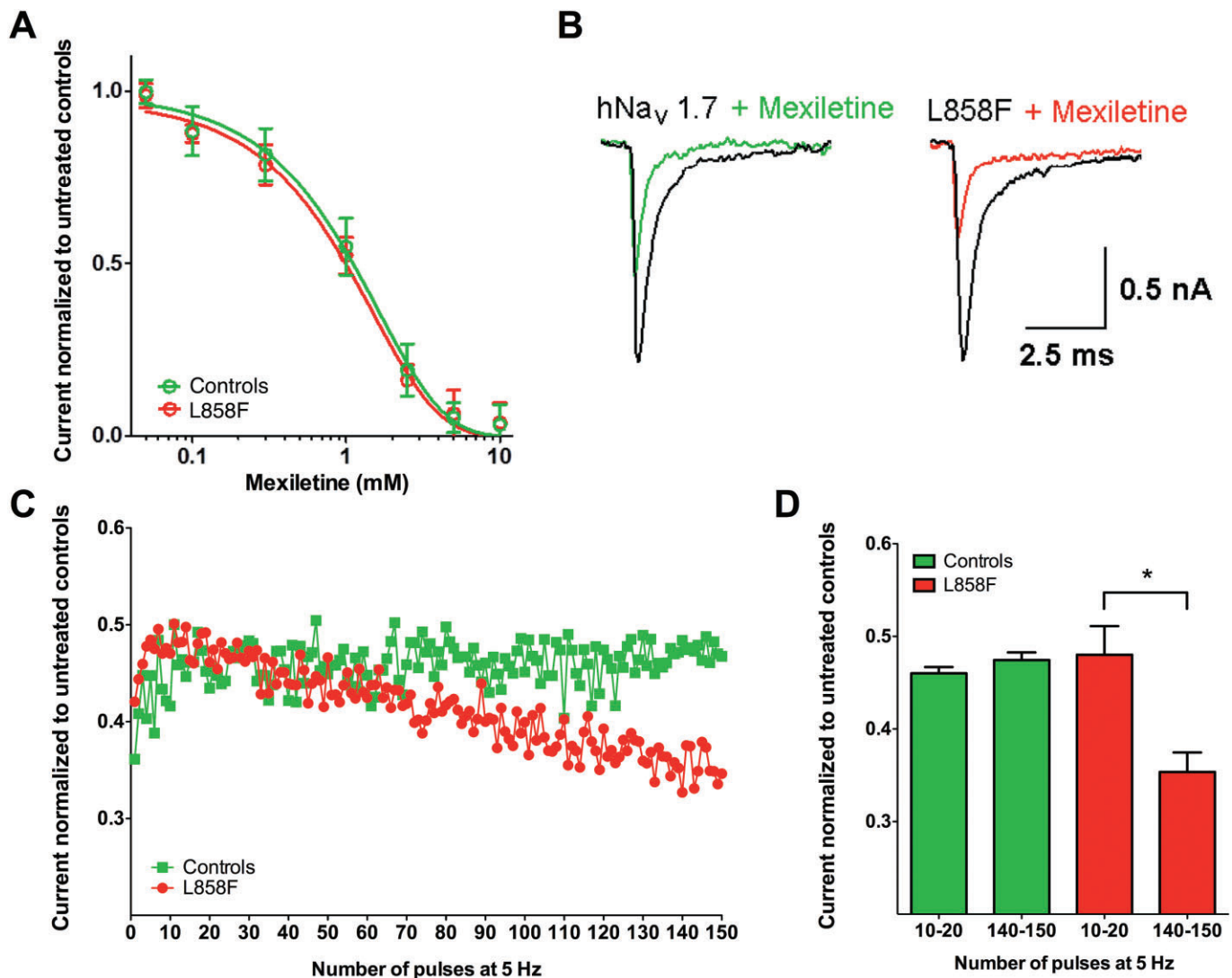
Figure 2

Concentration-dependent and use-dependent effects of mexiletine on Na$_V$1.7-mediated currents in HEK293 in whole-cell voltage-clamp configuration. (A) Concentration-dependent reduction in peak current by mexiletine in wild-type Na$_V$1.7 control channels and L858F channel mutation. Non-linear regression, calculated by plotting log-transformed inhibitor versus normalized response, generated IC$_{50}$ of 1.1 mM (0.05) for wild-type Na$_V$1.7 channels and 0.87 mM (0.06) for L858F mutant channels. (B) Representative examples of current traces before and during treatment with mexiletine (500 M) at the last depolarizing voltage step of a high-frequency stimulation protocol with 150 pulses at 5 Hz as described below. (C/D) Peak currents were normalized to maximum currents in untreated controls. Currents were elicited in whole-cell configuration by initially holding the cell at –120 mV and stepping up to 0 mV for 5 ms every 200 ms, generating pulses at a frequency of 5 Hz. While mexiletine (500 µM) led to a use-dependent fall-off in peak current for L858F, no use-dependent effect was found in controls with wild-type Na$_V$1.7 channels. All data are presented as means ± SEM (n = 8). One-way ANOVA and *post hoc* Bonferroni test; *P < 0.05.

of the steady-state fast inactivation was shifted to more hyperpolarized potentials in both the WT and mutant L858F channels to a similar degree. This effect substantially contributed to the reduction in the windows currents observed after treatment with mexiletine in L858F mutant channels. Although the effects of mexiletine have been investigated previously in another (V872G) Na$_V$1.7 mutation *in vitro*, where it was shown to induce use-dependent current blocking effects (Choi *et al.*, 2009), to our knowledge, this is the first evidence that the mechanism of action of mexiletine on erythromelalgia channel mutations involves an effect on their gating properties.

Furthermore, we observed that mexiletine induced a use-dependent inhibition of peak currents in the L858F mutant channels. A likely explanation for this phenomenon has been suggested by Waxman and co-workers (Choi *et al.*, 2009) when investigating another mutant channel. V872G was tested in similar conditions with high-frequency stimulation pulsing to –10 mV in the presence and absence of mexiletine. A stronger, use-dependent fall-off of current can be explained by a hyperpolarizing shift in activation of the mutant channel. Thus, a greater proportion of mutant channels will be opened and then inactivated during the early part of action potential generation. Once reaching +20 mV,
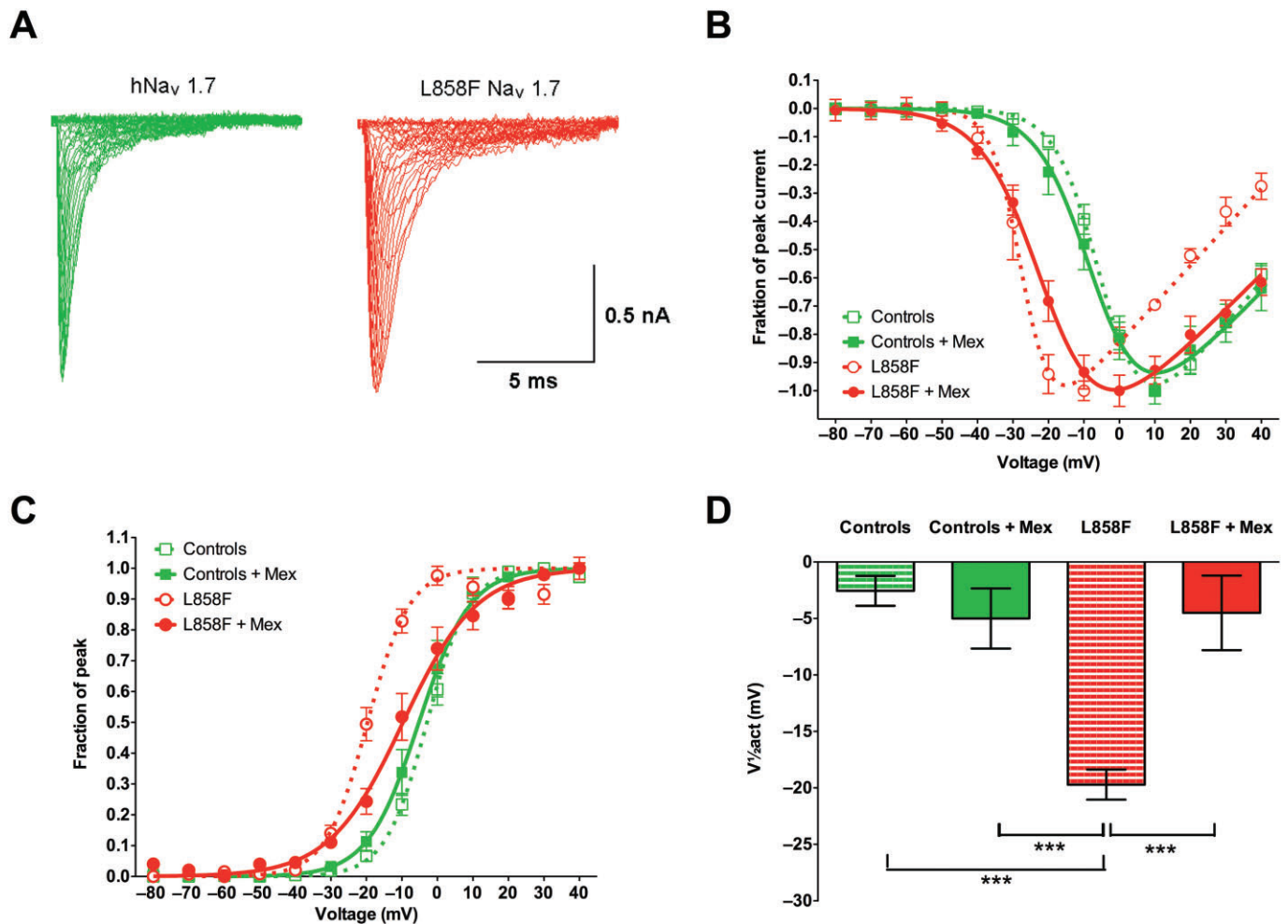
Figure 3
Voltage-dependence of steady-state activation of Na$_V$1.7-mediated currents in whole-cell voltage-clamp configuration. (A) Representative current traces recorded from HEK293A cells that expressed wild-type (left) or L858F mutant (right) Na$_V$1.7 together with hβ1 and hβ2. Whole-cell Na$^+$ currents were elicited by 10 ms test pulses with 5 s intervals to potentials between −80 and 40 mV in steps of 10 mV from a holding potential of −120 mV. (B) Current–voltage plot of wild-type Na$_V$1.7 (Controls), wild-type Na$_V$1.7 channels exposed to 500 μM mexiletine (Controls + Mex), L858F mutation (L858F) and L858F mutation exposed to 500 μM mexiletine (L858F + Mex). (C) Conductance values from HEK293 cells expressing wild-type Nav1.7 (Controls), wild-type Na$_V$1.7 channels exposed to 500 μM mexiletine (Controls + Mex), L858F mutants (L858F) and L858F mutants exposed to 500 μM mexiletine (were calculated from peak inward currents in activation protocols, normalized and fitted using the Boltzmann equation). (D) Analysis of voltages for half-maximal activation (V$_{1/2act}$) revealed a hyperpolarizing shift in the voltage-dependence of steady-state activation in L858F-expressing cells compared with controls. Mexiletine treatment of L858F-expressing cells, however, shifted the current-voltage relationship towards wild-type values, although a complete return to physiological values was not achieved. Please note that the mean data as used for statistical analysis do not entirely correspond to the graph depicted in panel (B) as these were fitted from averaged experimental results to demonstrate one representative graph for display purposes. All data presented are as means ± SEM; $n = 20$ for controls; $n = 9$ for controls exposed to mexiletine, $n = 15$ for L858F mutation and $n = 20$ for L858F mutation exposed to mexiletine. One-way ANOVA with *post hoc* Bonferroni test; ***$P < 0.001$.

activation of both V872G as well as WT channels is at its maximum. At −10 mV, however, it is possible for us to observe this effect. When comparing the use-dependent effect to tonic block, we also think that a frequency-dependent interaction between L858F and mexiletine may be the main reason why this drug, as well as other sodium channel blockers, is effective in PEM.

In a recent study of a gain-of-function mutation (M1476I) in Na$_V$1.4 (Zhao *et al.*, 2012), which is associated with cold-induced myotonia, effects on channel gating properties were

also observed, although mexiletine significantly shifted the voltage-dependent activation and inactivation curves of both WT and M1476I channels in a hyperpolarizing direction. In contrast, the voltage-dependence of activation in Na$_V$1.7 L858F channels was shifted in a depolarizing direction, whereas wild-type channels remained unaffected. In agreement with their findings, we found a hyperpolarizing shift in steady-state fast inactivation. Subtype-specific effects on voltage-gating properties of Na$_V$ have been found before, for example, for lidocaine (Chevrier *et al.*, 2004), which only
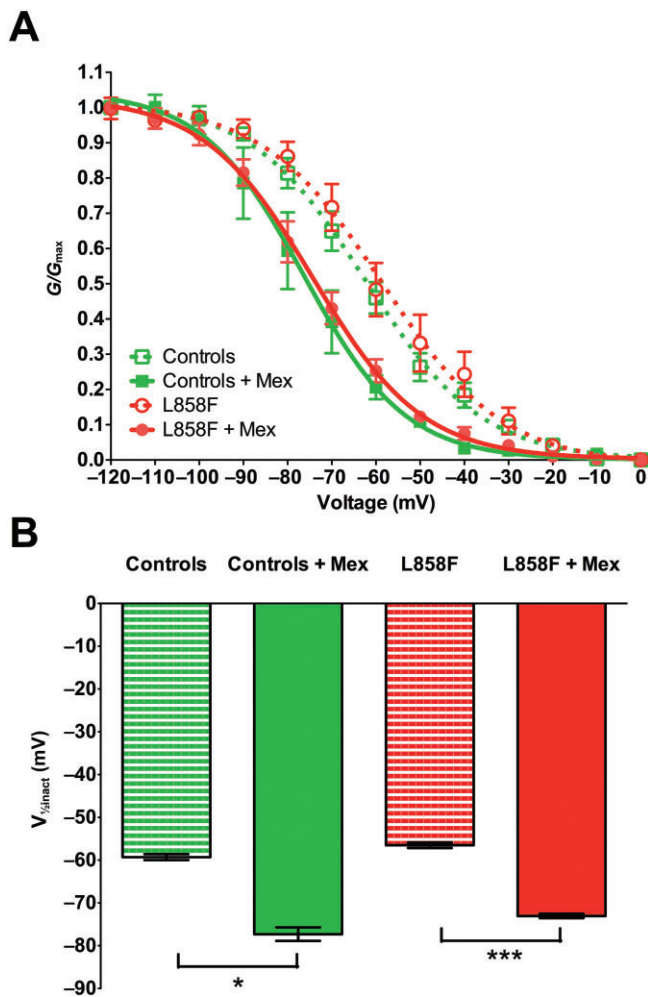
A

B

Figure 4

Voltage-dependence of steady-state fast inactivation of Na$_V$1.7-mediated currents in whole-cell voltage-clamp configuration. (A) Voltage-dependent inactivation in HEK293 cells expressing wild-typeNa$_V$1.7 (Controls), wild-type Na$_V$1.7 channels exposed to 500 µM mexiletine (Controls + Mex), L858F mutants (L858F) and L858F mutants exposed to 500 µM mexiletine (L858F + Mex) was assessed by holding the cells at potentials increasing from −120 to 0 mV for 500 ms, followed by a step to −10 mV for 50 ms, normalized to peak currents and fitted using the Boltzmann equation. (B) Analysis of voltages for half-maximal inactivation (V$_{1/2inact}$) in L858F-expressing cells and wild-type Na$_V$1.7 controls. A similar degree of hyperpolarizing shift in inactivation curves was observed in L858F mutant- and the wild-type Na$_V$1.7-expressing cells exposed to 500 µM mexiletine. Slope factors of the fitted curves did not differ between L858F mutants and wild-type Na$_V$1.7. All data are presented as means ± SEM; $n = 7$ for controls; $n = 5$ for controls exposed to mexiletine, $n = 19$ for L858F mutation and $n = 12$ for L858F mutation exposed to mexiletine. One-way ANOVA with *post hoc* Bonferroni test; *$P < 0.05$; ***$P < 0.001$.

shifts steady-state inactivation, but not activation in Na$_V$1.7, while both activation and inactivation were affected in Na$_V$1.8.

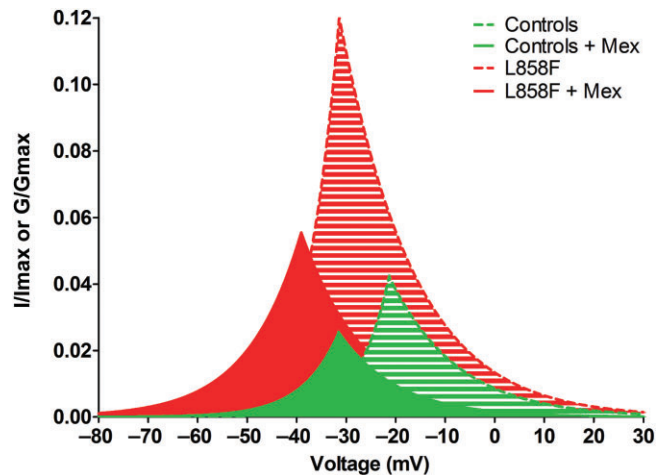It should be noted that the concentration of mexiletine found to be effective in the experiments described is much

Figure 5

Analysis of window currents in whole-cell voltage-clamp configuration of Na$_V$1.7-expressing HEK293 cells. Combined superimposed fitted curves of steady-state activation and fast inactivation kinetics in cells expressing Na$_V$1.7 channels (controls or L858F mutant) with Na$_V$β1 and Na$_V$β2 subunits. Window currents of cell population expressing wild-type channels (green striped area) were reduced by mexiletine (500 µM; green solid area). Mexiletine treatment (500 µM; red solid area) also reduced window currents of cells expressing L858F mutant channels (red striped area). All data are presented are as means.

higher than expected, based on the therapeutic concentrations active clinically. This may, in part, be explained by the simplified nature of the experiments, with cells highly overexpressing the investigated channel, acute wash-in of mexiletine rather than the slow accumulation that would in neuronal tissues *in vivo*, and the experiments were performed at lower ambient temperatures. A further reason may be related to the use-dependence of the drug, since in our experiments the membrane was held at a potential of −120 mV to remove steady-state inactivation. This may have resulted in a reduction in the blocking potency due to the unavailability of channels that would normally be open at the resting membrane potential of nociceptive neurons. Indeed, a reduction in the blocking potency of the same drug has already been described for voltage-gated sodium channels in skeletal muscle (Courtney, 1981). Nevertheless, the higher IC$_{50}$ values for the channel blocking actions of sodium channel blockers observed is very common for this type of experimental approach, as recently demonstrated for lidocaine (Sheets *et al.*, 2011).

Other medications that have been demonstrated to be of benefit in erythromelalgia patients have been previously investigated *in vitro* and responsiveness to treatment has been shown to be dependent on the exact causative mutation. For example, carbamazepine has been shown to normalize the hyperpolarizing shift in the voltage-dependence of activation produced by the V400M or S241T Na$_V$1.7 mutations but have no effect on the F1449V mutation (Fischer *et al.*, 2009; Yang *et al.*, 2012). Similar effects on the voltage-dependence of steady-state fast inactivation have been observed previously for carbamazepine, phenytoin and lamotrigine in WT

voltage-gated sodium channels in rat cultured cortical neurons (Errington *et al.*, 2008).

A further example of a substance with effects on voltage-gating properties of wild-type $Na_V1.7$ is the sea anemone peptide blood-depressing substance I (BDS-I), which was found to shift the voltage-dependence of both activation and inactivation towards more depolarized potentials. Furthermore, the authors also reported a change in the slope factor of the activation curve, an effect that we also observed for mexiletine in the L858F mutant channels (Liu *et al.*, 2012).

More recently, Wu and colleagues characterized three patients clinically diagnosed and confirmed to host EM-causative mutations in their *SCN9A* genes. Causative mutations were overexpressed in CHO cells, and IC_{50} values of lidocaine and mexiletine were compared with the mutations identified as I136V, I848T and V1316A (Wu *et al.*, 2013). They found differential effects between lidocaine and mexiletine, which were similar to the treatment effects observed in the affected patients.

Despite the almost complete normalization of activation properties in our case and tendency to normalization of repetitive firing current characteristics, a complete diminishment of the phenotypic aberrations affecting the sufferers of this rare but extremely debilitating painful disorder has not yet been reported. As recently proposed (Estacion *et al.*, 2011; Waxman, 2013), PEM symptoms might result from interactions between sympathetic and sensory neurons and so treatment modalities focused on altering neuronal excitability in the dorsal root ganglia alone may be either ineffective or only partially beneficial. Although mexiletine can provide some pain relief for erythromelalgia patients, it is by no means a cure for all. By understanding how mexiletine alters the biophysical properties of specific mutant $Na_V1.7$ channels, such as the one investigated in this study, we can potentially find new and better ways to normalize these biophysical properties and hopefully ameliorate pain.

Conclusions

In summary, our study demonstrates an example of predicting the treatment effect of mexiletine in patients suffering from a specific gain-of-function mutation in $Na_V1.7$. By applying the same *in vitro* approach to other PEM mutations, it might be possible to provide an informed prediction of the usefulness of mexiletine as a treatment for this rare inherited pain disorder.

Acknowledgements

Author contributions

R. C. conducted the experiments, analysed the data and wrote the manuscript. J. J. C. guided and supported the experiments, assessed the results and wrote the manuscript. D. L. H. B. assessed the results and wrote the manuscript. J. N. W. assessed the results and wrote the manuscript. R. W. conducted the experiments, analysed the data and wrote the manuscript.

Conflict of interest

None.

References

Alexander SPH, Benson HE, Faccenda E, Pawson AJ, Sharman JL, Spedding M, Peters JA and Harmar AJ, CGTP Collaborators. (2013). The Concise Guide to PHARMACOLOGY 2013/14: Ion channels. Br J Pharmacol 170: 1607–1646.

Challapalli V, Tremont-Lukats IW, McNicol ED, Lau J, Carr DB (2005). Systemic administration of local anesthetic agents to relieve neuropathic pain. Cochrane Database Syst Rev (4): CD003345.

Cheng X, Dib-Hajj SD, Tyrrell L, Te Morsche RH, Drenth JPH, Waxman SG (2011). Deletion mutation of sodium channel Na(V)1.7 in inherited erythromelalgia: enhanced slow inactivation modulates dorsal root ganglion neuron hyperexcitability. Brain 134: 1972–1986.

Chevrier P, Vijayaragavan K, Chahine M (2004). Differential modulation of Nav1.7 and Nav1.8 peripheral nerve sodium channels by the local anesthetic lidocaine. Br J Pharmacol 142: 576–584.

Chew CY, Collett J, Singh BN (1979). Mexiletine: a review of its pharmacological properties and therapeutic efficacy in arrhythmias. Drugs 17: 161–181.

Choi J-S, Zhang L, Dib-Hajj SD, Han C, Tyrrell L, Lin Z *et al.* (2009). Mexiletine-responsive erythromelalgia due to a new Na(v)1.7 mutation showing use-dependent current fall-off. Exp Neurol 216: 383–389.

Courtney KR (1981). Comparative actions of mexiletine on sodium channels in nerve, skeletal and cardiac muscle. Eur J Pharmacol 74: 9–18.

Cox JJ, Reimann F, Nicholas AK, Thornton G, Roberts E, Springell K *et al.* (2006). An SCN9A channelopathy causes congenital inability to experience pain. Nature 444: 894–898.

Dib-Hajj SD, Rush AM, Cummins TR, Hisama FM, Novella S, Tyrrell L *et al.* (2005). Gain-of-function mutation in Nav1.7 in familial erythromelalgia induces bursting of sensory neurons. Brain 128: 1847–1854.

Ebell MH (2006). Systemic lidocaine or mexiletine for neuropathic pain. Am Fam Physician 74: 79.

Errington AC, Stöhr T, Heers C, Lees G (2008). The investigational anticonvulsant lacosamide selectively enhances slow inactivation of voltage-gated sodium channels. Mol Pharmacol 73: 157–169.

Estacion M, Han C, Choi J-S, Hoeijmakers JGJ, Lauria G, Drenth JPH et al. (2011). Intra- and interfamily phenotypic diversity in pain syndromes associated with a gain-of-function variant of NaV1.7. Mol Pain 7: 92.

Fenster PE, Comess KA (1986). Pharmacology and clinical use of mexiletine. Pharmacotherapy 6: 1–9.

Fischer TZ, Gilmore ES, Estacion M, Eastman E, Taylor S, Melanson M et al. (2009). A novel Nav1.7 mutation producing carbamazepine-responsive erythromelalgia. Ann Neurol 65: 733–741.

Han C, Rush AM, Dib-Hajj SD, Li S, Xu Z, Wang Y et al. (2006). Sporadic onset of erythermalgia: a gain-of-function mutation in Nav1.7. Ann Neurol 59: 553–558.

Han C, Lampert A, Rush AM, Dib-Hajj SD, Wang X, Yang Y et al. (2007). Temperature dependence of erythromelalgia mutation L858F in sodium channel Nav1.7. Mol Pain 3: 3.

Jarvis B, Coukell AJ (1998). Mexiletine. A review of its therapeutic use in painful diabetic neuropathy. Drugs 56: 691–707.

Kuhnert SM, Phillips WJ, Davis MD (1999). Lidocaine and mexiletine therapy for erythromelalgia. Arch Dermatol 135: 1447–1449.

Legroux-Crespel E, Sassolas B, Guillet G, Kupfer I, Dupre D, Misery L (2003). [Treatment of familial erythermalgia with the association of lidocaine and mexiletine]. Ann Dermatol Venereol 130: 429–433.

Liu P, Jo S, Bean BP (2012). Modulation of neuronal sodium channels by the sea anemone peptide BDS-I. J Neurophysiol 107: 3155–3167.

Mao J, Chen LL (2000). Systemic lidocaine for neuropathic pain relief. Pain 87: 7–17.

Marmura MJ (2010). Intravenous lidocaine and mexiletine in the management of trigeminal autonomic cephalalgias. Curr Pain Headache Rep 14: 145–150.

Matthews E, Fialho D, Tan SV, Venance SL, Cannon SC, Sternberg D et al. (2010). The non-dystrophic myotonias: molecular pathogenesis, diagnosis and treatment. Brain 133: 9–22.

Middleton D (1980). Baseline pharmacology, electrophysiology and pharmacokinetics of mexiletine. Acta Cardiol Suppl: 45–53.

Monk JP, Brogden RN (1990). Mexiletine. A review of its pharmacodynamic and pharmacokinetic properties, and therapeutic use in the treatment of arrhythmias. Drugs 40: 374–411.

Nathan A, Rose JB, Guite JW, Hehir D, Milovcich K (2005). Primary erythromelalgia in a child responding to intravenous lidocaine and oral mexiletine treatment. Pediatrics 115: e504–e507.

Pawson AJ, Sharman JL, Benson HE, Faccenda E, Alexander SP, Buneman OP, Davenport AP, McGrath JC, Peters JA, Southan C, Spedding M, Yu W, Harmar AJ; NC-IUPHAR. (2014). The IUPHAR/BPS Guide to PHARMACOLOGY: an expert-driven knowledgebase of drug targets and their ligands. Nucl. Acids Res 42 (Database Issue): D1098–106.

Samuels ME, te Morsche RHM, Lynch ME, Drenth JPH (2008). Compound heterozygosity in sodium channel Nav1.7 in a family with hereditary erythermalgia. Mol Pain 4: 21.

Segerdahl AR, Xie J, Paterson K, Ramirez JD, Tracey I, Bennett DLH (2012). Imaging the neural correlates of neuropathic pain and pleasurable relief associated with inherited erythromelalgia in a single subject with quantitative arterial spin labelling. Pain 153: 1122–1127.

Sheets PL, Jarecki BW, Cummins TR (2011). Lidocaine reduces the transition to slow inactivation in Na(v)1.7 voltage-gated sodium channels. Br J Pharmacol 164: 719–730.

Statland JM, Bundy BN, Wang Y, Rayan DR, Trivedi JR, Sansone VA et al. (2012). Mexiletine for symptoms and signs of myotonia in nondystrophic myotonia: a randomized controlled trial. JAMA 308: 1357–1365.

Tremont-Lukats IW, Challapalli V, McNicol ED, Lau J, Carr DB (2005). Systemic administration of local anesthetics to relieve neuropathic pain: a systematic review and meta-analysis. Anesth Analg 101: 1738–1749.

Waxman SG (2013). Painful Na-channelopathies: an expanding universe. Trends Mol Med 19: 406–409.

Woosley RL, Wang T, Stone W, Siddoway L, Thompson K, Duff HJ et al. (1984). Pharmacology, electrophysiology, and pharmacokinetics of mexiletine. Am Heart J 107: 1058–1065.

Wu M-T, Huang P-Y, Yen C-T, Chen C-C, Lee M-J (2013). A novel SCN9A mutation responsible for primary erythromelalgia and is resistant to the treatment of sodium channel blockers. PLoS ONE 8: e55212.

Yang Y, Dib-Hajj SD, Zhang J, Zhang Y, Tyrrell L, Estacion M et al. (2012). Structural modelling and mutant cycle analysis predict pharmacoresponsiveness of a Na(V)1.7 mutant channel. Nat Commun 3: 1186.

Zhao J, Duprè N, Puymirat J, Chahine M (2012). Biophysical characterization of M1476I, a sodium channel founder mutation associated with cold-induced myotonia in French Canadians. J Physiol (Lond) 590: 2629–2644.